A Simulation Method for the One-time Snap-fit Assembly Process of PA6 GF60 - Components

Nicolae Stefanoaea
Faculty of Engineering, Lucian Blaga University of Sibiu, Romania
nicolae.stefanoaea@ulbsibiu.ro

Dan-Mihai Rusu
Faculty of Engineering, Lucian Blaga University of Sibiu, Romania
dan-mihai.rusu@ulbsibiu.ro (corresponding author)

Adrian-Marius Pascu
Faculty of Engineering, Lucian Blaga University of Sibiu, Romania
adrian.pascu@ulbsibiu.ro

Received: 7 December 2023 | Revised: 27 December 2023 | Accepted: 6 January 2024

 DOI: https://doi.org/10.48084/etasr.6715

ABSTRACT

This paper's scope is to develop an intelligible Finite Element Analysis (FEA) method, utilized to determine and quantify the assembly forces required to assemble the snap-fit component, which is made of a glass fiber reinforced polyamide (type 6, 60% glass fiber, PA6 GF50), as well as to determine the snap-fit joint maximum retention forces. The proposed FEA method is to be used in Abaqus as a standard solver type, considering its operation ease and simplicity in creating the model. The setback of implementing the standard solver approach is that during the snap-fit assembly, at a certain point in the simulation, the behavior is transformed from a static movement to a dynamic one, precisely when the snap moves backward in the assembled position, at this point, due to the dynamic behavior of the simulation, the solution will continue to diverge, and the convergence is not achieved.

Keywords-snap-fit; standard solver; abaqus; polyamide; glass fiber reinforced

I. INTRODUCTION

The automotive industry is in a continuous development regarding the reduction of the cost [1], the component weight [2], the time spent on the production line, and the complexity of the assembled components, leading to a decrease in the exhaust emissions of internal combustion engine cars [3]. To achieve this, car manufacturers and the automotive suppliers of the components played a crucial role. Additionally, the quantity of the metal and metal alloys [4] used was reduced and replaced with innovative plastics, [5] such as polyamides reinforced with glass fiber. Finally, instead of assembling the components via screws to the snap-fit clips, components made of reinforced glass fiber polyamides were developed. The snap-fit [6] clip assembly process offers the possibility of streamlining the industrial assembly procedures in which the automotive industry is heavily involved. The reason is that the former method has several advantages, namely assembly or disassembly speed, and construction simplicity, due to which automation can be quickly and easily realized [7]. As far as snap-fit assemblies are concerned, the more recent literature does not offer an extensive range of different outlooks on them. However, an important part of the researchers' concerns is related to resolving some dimensional limitations of parts made by engaging Additive Manufacturing (AM) technology as well as settling design issues. In the case of making parts larger than the workspace of 3D printers, researchers propose a solution whereby that part is divided into smaller ones and accumulated by these types of cheap and fast assemblies [8-10]. Also, in the context of quick-release assemblies in AM, authors in [11] conducted an experimental study on the determination of the required mating/dismounting force as a function of several predefined parameters. The experimental data were processed and compared with an analytical model expressed by a derived equation. Another perspective pinpointed in the literature is related to the identification of efficient robotic assembly methods using snap-fit elements. Unlike an assembly performed by a human operator, who validates it following an acoustic signal produced when the two parts have been collected, this is a challenge in robotic assembly. To meet this challenge, authors in [12] proposed a machine-learning method based on data obtained from force variation during the assembly process. Authors in [13] investigated the aspects of preload and stiffness factors as a technique of determining a complete and correct collection of snap-fit assemblies with seals or elastic gaskets where pre-tensioning is required. An even higher holding force and a higher engagement signal were found to lead to an increase in assembly confidence.

II. MATERIAL SELECTION

To be able to develop a simulation method that will provide results as close to reality as possible/credible results, a need for a good material definition has emerged. The input data for the material are chosen from [14]. Moreover, the same type of polyamide as the real component with the same amount of reinforcement material, in this case glass fiber, is selected. The material curve chosen from CAMPUS is shown in Figure 1.

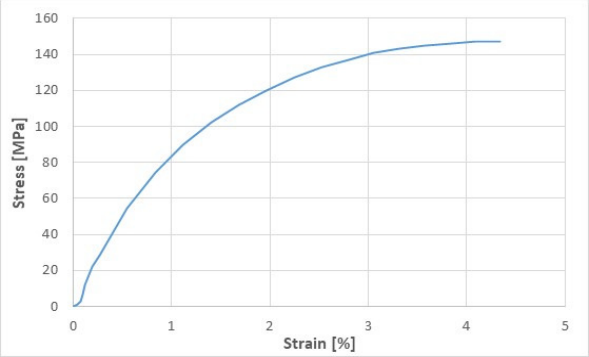

Fig. 1. Raw data input for the material definition in Abaqus.

The stress–strain curve out of campus is evaluated as engineering stress–strain. To be used in the FEA [15, 16], it is required to be transformed into true form [17]. For this reason, the equations shown below are performed to obtain the input data for the FEA analysis.

$$\frac{F}{S} = \sigma \quad (1)$$

$$ln\frac{L}{L_0} = \mathcal{E} \quad (2)$$

$$\frac{F}{S_0} = \sigma_{eng} \quad (3)$$

$$\frac{l-l_0}{l_0} = \varepsilon_{eng} \quad (4)$$

where F is the tensile force, s is the instantaneous section area, s_0 is the initial section area, l is the instantaneous length of the specimen, and l_0 is the initial length of the specimen.

The final material curve [18] that will be used in the FEA is illustrated in Figure 2.

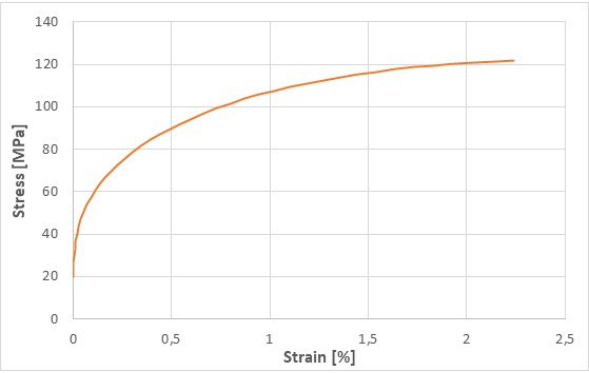

Fig. 2. True stress–strain curve for PA6 GF60.

III. SIMULATION METHOD

The simulation software utilized for determining the assembly forces as well as the maximum retention [19] force is Abaqus [20]. The simulation is formed employing two components: the snap-fit, as a deformable component and the body used as an analytical rigid component [21]. Nevertheless, in real life, the most substantial deformations occur only on the snap and no significant ones take place on the counterpart, while material data are considered for a non-linear simulation [22]. In Figure 3, the assembly is demonstrated. For a better solution convergence, the parts are arranged in direct contact [23], while no gap is preferred. The simulation is divided into 3 steps, shown in Figure 4. Regarding the boundary conditions, the snap is considered fixed in the bottom side whereas the body is free to move along the vertical axes. This is shown in Figure 5.

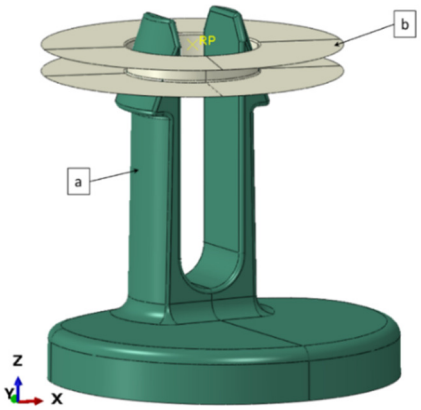

Fig. 3. 3D models of components prepared for the FEA: (a) Snap, (b) body.

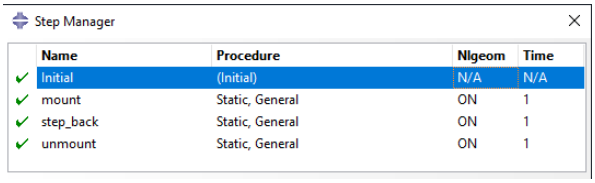

Fig. 4. Simulation steps.

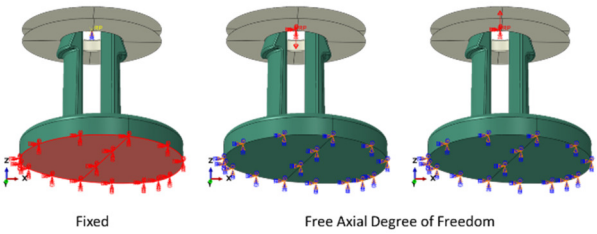

Fig. 5. Boundary conditions.

The main challenge for this type of simulation is to allow the snap to spring back into the assembled position while still using the Abaqus standard solver, while the resultant of the forces should be 0 throughout the steps. During the spring back into the final state moment, there is an instant force drop. So,

the solution goes from static to dynamic and the equilibrium equation of the standard solver will start to diverge. One quick solution is to use the Abaqus Explicit [24] solver, but in this case, the approach is not to be followed due to the simulation complexity. To prevent this, the total snap travel, up to the point where it is fixed to the the axial travel end, is split in half: in the first half the snap is radially deformed until the middle of the body height. In this way, it is ensured that the maximum assembly force is reached, considering the surface quality of the reinforced plastic components, that the resulting friction between the parts is low, and that the given force can be neglected. The second half, however, is formed when the contact between the snap and body is removed while keeping the displacement imposed. By removing the contact, the resulting force of the complete movement is 0. A detailed view of how this interaction is composed is demonstrated in Figure 6. In the final step, the direction of the body displacement is reversed in order to quantify the maximum retaining force of the snap. In this step, the contact between the body and the lower flat surface of the snap is defined, as spotted in Figure 7.

Interaction Manager

Name	Initial	mount	step_back	unmount
✓ body-snap-assembly	Created	Propagated	Deactivated	
✓ body-snap-disassembly				Created

Fig. 6. Simulation interacion based on simulation steps.

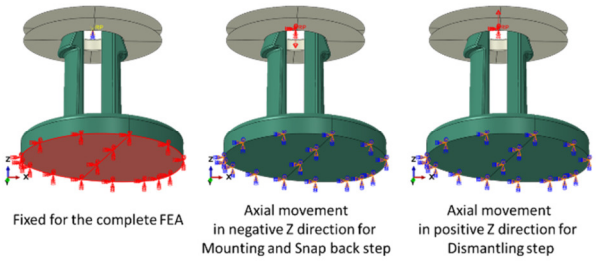

Fig. 7. Displacement boundary condition formulation.

IV. TEST METHOD

The test entails using a snap-fit of an automotive component onto the chassis, as it is observed in Figure 8. Considering that the chassis is too big to fit onto a small test rig, a similar fixture is built while retaining the geometry conditions close to reality, as shown in the test setup in Figure 9. The test is conducted using an Instron 5544 in displacement, which is controlled by employing an imposed displacement of 10 mm/min. The body is moved downwards until the snap is fully seated (the force drops to 0 N). For the maximum retention force, the body is moved upwards until the snap is not assembled, it is either sheared or slips out of the assembly.

V. SIMULATION – TEST COMPARISON

Based on the simulation, two forces are calculated by plotting the field output, the reaction force and displacement of the body reference point. For the first two steps, the output is the maximum assembly force of the snap. A direct comparison between simulation and test is presented in Figure 10.

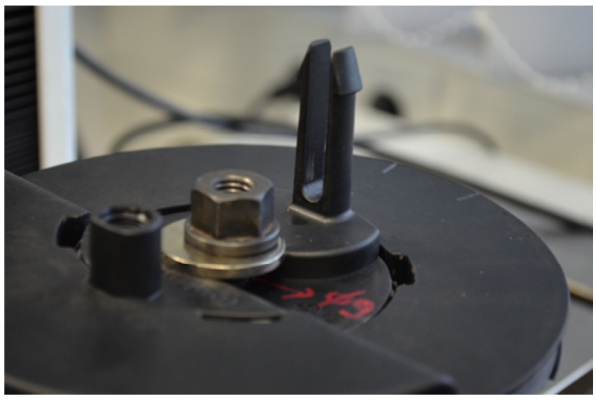

Fig. 8. Test component – snap fixture.

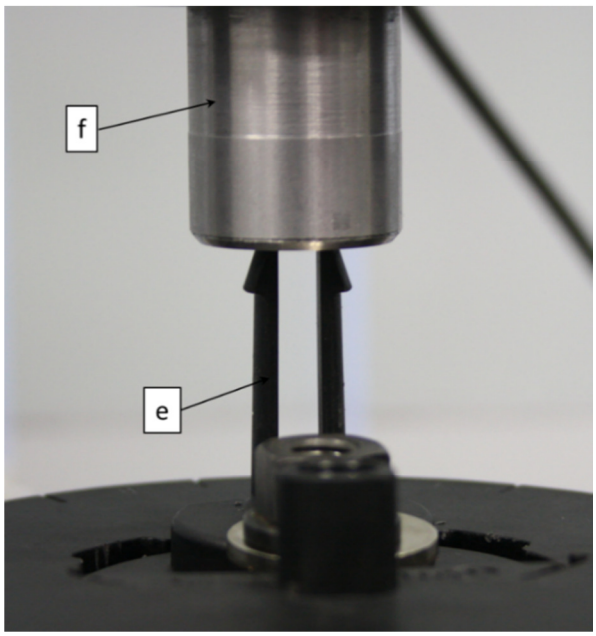

Fig. 9. Test Setup, (e) snap, (f) body.

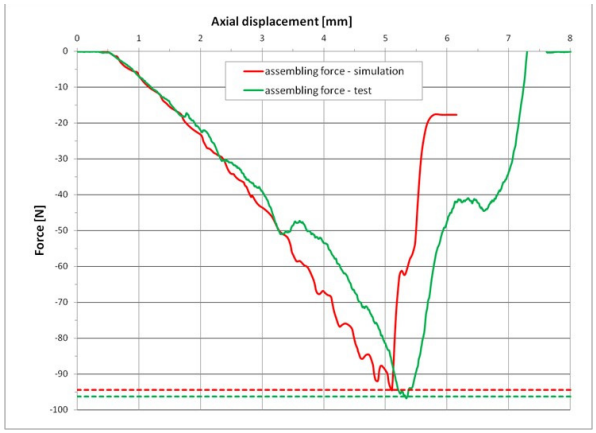

Fig. 10. Maximum assembly force. Green: test, red: simulation.

For the third step, the output is directly correlated with the results derived from the test. The displacement where the snap

shearing occurs in the test is considered to be the critical part of the simulation point, when evaluating the maximum retention force of the snap-fit and is identified in Figure 11. The critical stress value from the FEA is compared and evaluated for the maximum radial displacement and the simulation results are shown in Figure 12.

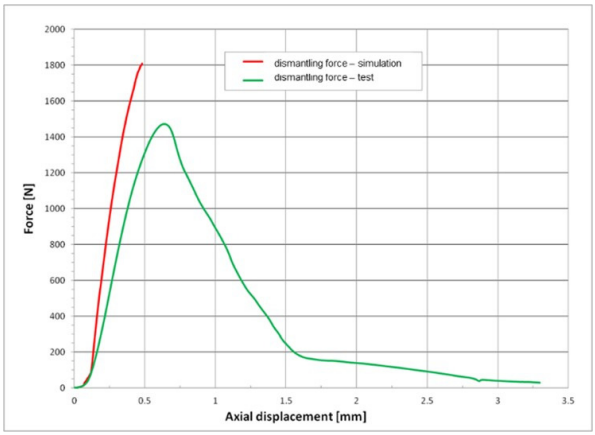

Fig. 11. Maximum retention force. Green: test, red: simulation.

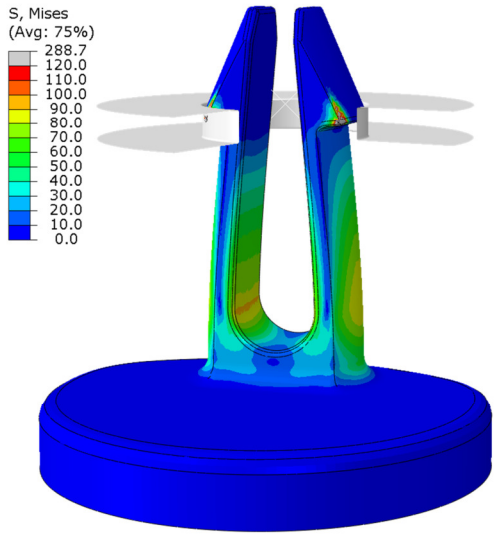

Fig. 12. Critical assembly stress value.

The critical stress value is evaluated for the limit where the material slope goes horizontal and thus the material starts to stretch. The stress in the corner of Figure 13, namely those above the imposed limit, are compressive stresses, and in this specific case, are not considered dangerous while evaluating the snap during the mounting step. For the dismantling step, a direct comparison of the snap stresses is made at the point where the shear of the snap occurs in reality. The results of the disassembly phase simulation in Abaqus can be seen in Figure 14. For the assessment of real situations [25], Figure 15 depicts the failure mode comparison in the test (a) and provides a detailed view of the critical area from the simulation (b).

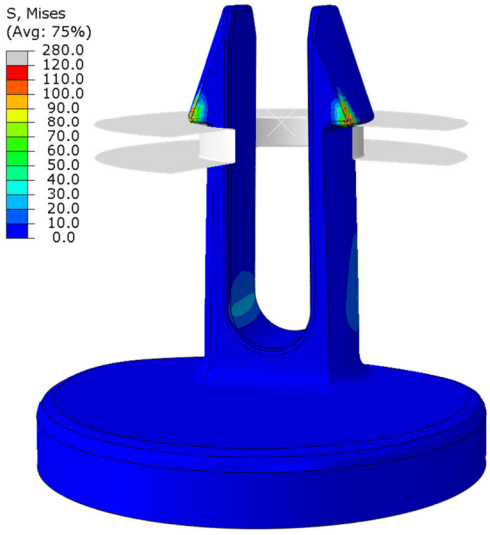

Fig. 13. Stress in assembled position.

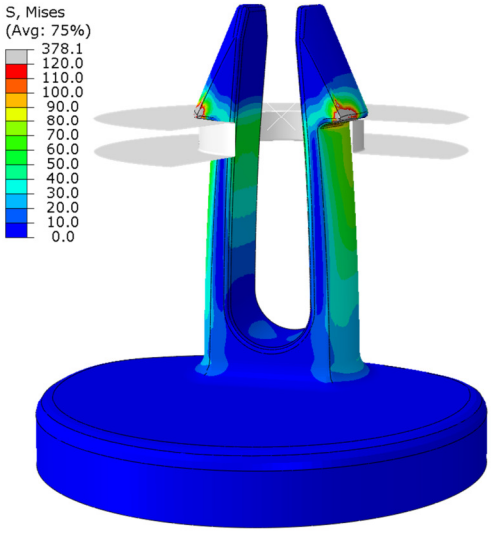

Fig. 14. Critical stress level for dismantling step.

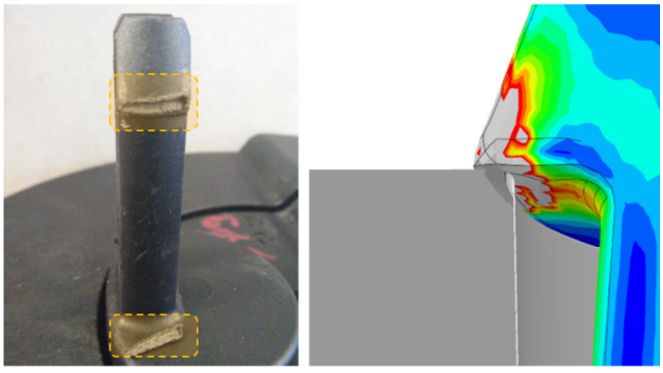

(a) (b)

Fig. 15. (a) Failure mode in test, (b) detailed view in the simulation.

VI. CONCLUSION AND FUTURE DEVELOPMENT

In the present work, the behavior of snap-fit assemblies was analyzed through numerical methods using numerical simulation tools. This analysis was carried out in order to reach a better understanding of the dynamic behavior of snap-fit assemblies, which is in line with the current concerns of the scientific community. Through the performed numerical simulations and the introduction of an intermediate step during the assembly simulation, after reaching the maximum radial displacement of the snap (maximum assembly force), the contact between the snap and the counterpart (the body) helps keeping the Abaqus standard as a solver. At the same time, this contact increases confidence for future results while the assembly force can be quantified. If needed, the parts can be optimized so that the assembly force is eliminated, reducing the cost and time invested into the assembly tools.

Future developments are required to establish a better evaluation of the critical point in the simulation when we can predict the snap out or the shearing of the plastic snaps. The next steps to follow concern the acquisition of ISO527 [26] tensile dog bone [27] samples, with fiber orientation distributed either along the tensile direction or perpendicularly to it, ideally built from the same supplier of the real component. Furthermore, stress estimation is expected to be obtained. The latter refers to strain data derived by applying a tensile test on them. With the resulting stress–strain data, the same method of obtaining the true form [17], employed in the FEA, can be used. In addition, a critical failure point can be chosen based on the tensile results. In this case, the test data are not necessary to establish the critical point.

REFERENCES

[1] D. Jasinski, J. Meredith, and K. Kirwan, "A comprehensive review of full cost accounting methods and their applicability to the automotive industry," *Journal of Cleaner Production*, vol. 108, pp. 1123–1139, Dec. 2015, https://doi.org/10.1016/j.jclepro.2015.06.040.

[2] *Global Analysis of Weight Reduction Strategies of Major OEMs*. Frost & Sullivan, 2009.

[3] Q. B. Jamali *et al.*, "Analysis of CO2, CO, NO, NO2, and PM Particulates of a Diesel Engine Exhaust," *Engineering, Technology & Applied Science Research*, vol. 9, no. 6, pp. 4912–4916, Dec. 2019, https://doi.org/10.48084/etasr.3093.

[4] N. Baluch, Z. M. Udin, and C. S. Abdullah, "Advanced High Strength Steel in Auto Industry: an Overview," *Engineering, Technology & Applied Science Research*, vol. 4, no. 4, pp. 686–689, Aug. 2014, https://doi.org/10.48084/etasr.444.

[5] E. Ghassemieh, "Materials in Automotive Application, State of the Art and Prospects," in *New Trends and Developments in Automotive Industry*, M. Chiaberge, Ed. IntechOpen, 2011, https://doi.org/10.5772/13286.

[6] P. R. Bonenberger, *The First Snap-Fit Handbook : Creating Attachments for Plastics Parts*. Munich, Germany: Hanser Gardner Pubns, 2000.

[7] R. W. Messler, S. Genc, and G. A. Gabriele, "Integral attachment using snap-fit features: a key to assembly automation. Part 1 - introduction to integral attachment using snap-fit features," *Assembly Automation*, vol. 17, no. 2, pp. 143–155, Jan. 1997, https://doi.org/10.1108/01445159710171365.

[8] J. L. Amaya, E. A. Ramírez, G. F. Maldonado, and J. Hurel, "Detailed design process and assembly considerations for snap-fit joints using additive manufacturing," *Procedia CIRP*, vol. 84, pp. 680–687, Jan. 2019, https://doi.org/10.1016/j.procir.2019.04.271.

[9] E. A. Ramírez, F. Caicedo, J. Hurel, C. G. Helguero, and J. L. Amaya, "Methodology for design process of a snap-fit joint made by additive manufacturing," *Procedia CIRP*, vol. 79, pp. 113–118, Jan. 2019, https://doi.org/10.1016/j.procir.2019.02.021.

[10] C. Klahn, D. Singer, and M. Meboldt, "Design Guidelines for Additive Manufactured Snap-Fit Joints," *Procedia CIRP*, vol. 50, pp. 264–269, Jan. 2016, https://doi.org/10.1016/j.procir.2016.04.130.

[11] K. Torossian and D. Bourell, "Experimental Study of Snap-Fits Using Additive Manufacturing," in *Proceedings for the 2015 International Solid Freeform Fabrication Symposium*, Austin TX, USA, Aug. 2015, Accessed: Jan. 11, 2024.

[12] S. Doltsinis, M. Krestenitis, and Z. Doulgeri, "A Machine Learning Framework for Real-Time Identification of Successful Snap-Fit Assemblies," *IEEE Transactions on Automation Science and Engineering*, vol. 17, no. 1, pp. 513–523, Jan. 2020, https://doi.org/10.1109/TASE.2019.2932834.

[13] L. Rusli, A. Luscher, and C. Sommerich, "Force and tactile feedback in preloaded cantilever snap-fits under manual assembly," *International Journal of Industrial Ergonomics*, vol. 40, no. 6, pp. 618–628, Nov. 2010, https://doi.org/10.1016/j.ergon.2010.05.005.

[14] "CAMPUSplastics." https://www.campusplastics.com/.

[15] "Finite element method," *Wikipedia*. Jan. 10, 2024, [Online]. Available: https://en.wikipedia.org/w/index.php?title=Finite_element_method&oldid=1194758633.

[16] "About FEM," *University of Birmingham*. https://intranet.birmingham.ac.uk/collaboration/hpc-research/abaqus-sig/about/index.aspx.

[17] X. W. Du, G. J. Sun, and C. Nie, "A Method to Calculate the True Stress and True Strain for Tensile Test of Plastic," *Key Engineering Materials*, vol. 274–276, pp. 1077–1082, 2004, https://doi.org/10.4028/www.scientific.net/KEM.274-276.1077.

[18] T. Dalrymple, "Material Model Calibration App in 3DEXPERIENCE Platform," *Dassault Systèmes blog*, Jan. 17, 2019. https://blog.3ds.com/brands/simulia/material-model-calibration-app-3dexperience-platform/.

[19] X.-L. Guo and B.-H. Sun, "Assembly and disassembly mechanics of a spherical snap fit," *Theoretical and Applied Mechanics Letters*, vol. 13, no. 1, Jan. 2023, Art. no. 100403, https://doi.org/10.1016/j.taml.2022.100403.

[20] *"Abaqus 2021." Dassault Systèmes*, 2021, [Online]. Available: https://www.3ds.com/support/hardware-and-software/simulia-system-information/abaqus-2021/test-configurations-for-abaqus-2021/.

[21] P. Golewski and T. Sadowski, "Numerical Analysis of Two Types Polymeric Fibre Composite Materials with Different Reinforcement Architecture for Creation of Innovative Snap-fit Joints," *IOP Conference Series: Materials Science and Engineering*, vol. 416, no. 1, Jun. 2018, Art. no. 012061, https://doi.org/10.1088/1757-899X/416/1/012061.

[22] "2.2.1 Nonlinear solution methods in ABAQUS/Standard," *ABAQUS Theory Manual (v6.6)*. https://classes.engineering.wustl.edu/2009/spring/mase5513/abaqus/docs/v6.6/books/stm/default.htm?startat=ch02s02ath14.html.

[23] *Modeling Contact with Abaqus/Standard*. Dassault Systèmes, 2018.

[24] Experts Of CAE Assistant Group, "Differences Between ABAQUS Standard & ABAQUS Explicit," *CAE Assistant*, Feb. 21, 2020. https://caeassistant.com/blog/abaqus-standard-or-abaqus-explicit/.

[25] G. Suri, "A Fundamental Investigation of Retention Phenomena in Snap-fit Features," Ph.D. dissertation, The Ohio State University, Columbus, OH, USA, 2002.

[26] "ISO 527-1:2019. Plastics. Determination of tensile properties." ISO, 2019.

[27] D. G. Zisopol, A. I. Portoaca, and M. Tanase, "Dimensional Accuracy of 3D Printed Dog-bone Tensile Samples: A Case Study," *Engineering, Technology & Applied Science Research*, vol. 13, no. 4, pp. 11400–11405, Aug. 2023, https://doi.org/10.48084/etasr.6060.